A EUROPEAN JOURNAL OF CHEMICAL BIOLOGY

CHEMBIOCHEM

SYNTHETIC BIOLOGY & BIO-NANOTECHNOLOGY

Accepted Article

Title: Mechanism of diol dehydration by a promiscuous radical-SAM enzyme homologue of the antiviral enzyme viperin (RSAD2)

Authors: Kourosh Honarmand Ebrahimi, Jack Rowbotham, James McCullagh, and William S James

To be cited as: *ChemBioChem* 10.1002/cbic.201900776

Link to VoR: http://dx.doi.org/10.1002/cbic.201900776

A Journal of

ChemPubSoc Europe

WILEY-VCH

www.chembiochem.org

RESEARCH ARTICLE WILEY-VCH

Mechanism of diol dehydration by a promiscuous radical-SAM enzyme homologue of the antiviral enzyme viperin (RSAD2)

Kourosh Honarmand Ebrahimi*[a], Jack S. Rowbotham[a], James McCullagh[a], William S. James[c]

[a] Dr Kourosh H. Ebrahimi, Dr Jack S. Rowbotham, Prof James McCullagh
Department of Chemistry
University of Oxford
Chemistry Research Laboratory, Mansfield Road, OX1 3TA, Oxford, UK
E-mail: Kourosh.honarmandebrahimi@chem.ox.ac.uk
[b] Prof William S. James
Sir William Dunn School of Pathology
University of Oxford
South Parks Road, OX1 3RE, Oxford, UK

Supporting information for this article is given via a link at the end of the document.((Please delete this text if not appropriate))

Abstract: 3′-deoxy nucleotides are an important class of drugs because they interfere with the metabolism of nucleotides and their incorporation into DNA or RNA terminates cell division and viral replication. These compounds have largely been produced via multistep chemical synthesis and an enzyme with the ability to catalyse the removal of the 3′-deoxy group from different nucleotides has yet to be described. Here, using a combination of HPLC, high-resolution mass spectrometry, and NMR spectroscopy we demonstrate that a thermostable fungal radical S-adenosylmethionine (SAM) enzyme with similarity to the vertebrate antiviral enzyme viperin (RSAD2) can catalyze transformation of CTP, UTP, and 5-bromo-UTP to their 3'-deoxy-3′,4'-didehydro analogues. We show that unlike the fungal enzyme, human viperin can only catalyse the transformation of CTP. Using electron paramagnetic resonance (EPR) spectroscopy and molecular docking and dynamics simulations in combination with mutagenesis studies we provide insight into the origin of the unprecedented substrate promiscuity of the enzyme and the mechanism of dehydration of a nucleotide. Our findings highlight the evolution of substrate specificity in a member of the radical-SAM enzymes. We predict that our work will help in utilizing a new class of radical-SAM enzymes for biocatalytic synthesis of 3'-deoxy nucleotide/nucleoside analogues.

Introduction

Currently there are more than 25 nucleotide/nucleoside analogues approved as antiviral or anticancer medications and there are several more at different stages of preclinical development[1,2]. Additionally, new analogues with antibacterial activity have been discovered[3]. Among different analogues, those missing the 3'-hydroxyl group interfere with metabolism of nucleotides, which are the building blocks of DNA and RNA, or terminate activity of RNA or DNA polymerases. Consequently, they halt reproduction of pathogens or cancer cells[1,3]. Examples include the antiviral drug telbivudine, which is a uridine analogue used to treat hepatitis B infection[4], and the nucleoside analogue 3'-deoxy-3′,4'-didehydro-cytidine (ddhC), which is predicted to have cytotoxic and anticancer properties[5]. While nucleoside phosphorylases have been shown to catalyse synthesis of a wide range of nucleotide/nucleoside analogues by transferring a nitrogenous base mainly to ribose or 2′-modified ribose[6–9], an enzymatic method for direct conversion of different nucleotides to their 3'-deoxy form will present many new opportunities for developing biobased medications. This is because chemical synthesis methods consisting of multiple protection-deprotection steps in organic solvents, are time consuming, need high temperatures, and generate different side products and toxic wastes[10,11].

Members of the radical-SAM superfamily of enzymes are emerging as important biocatalysts in biosynthetic routes to sugar-containing natural products for treatment of infectious diseases[12–15]. The radical-SAM addition reactions using NosL are proposed as an effective way to synthesize nucleoside-containing compounds[16]. More recently, it has been demonstrated that the vertebrate antiviral radical-SAM enzyme viperin (RSAD2) can catalyse modification of ribose moiety in CTP and its conversion to 3′-deoxy-3′,4′-didehydro-CTP (ddhCTP)[17]. It is shown that Rattus norvegicus viperin has substrate specificity and can only catalyse transformation of CTP among other nucleotides[17].

We have investigated a new member of the radical-SAM superfamily of enzymes from the thermophilic fungus *Thielavia terrestris* with similarity to the human antiviral enzyme viperin (RSAD2). Thus, we named the enzyme TtRSAD2. We demonstrate that this enzyme has substrate promiscuity unlike human viperin. We show that while TtRSAD2 catalyses transformation of CTP, UTP, and 5-bromo-UTP to their 3′-deoxy-3′,4′-didehydro analogues, human viperin can only catalyse transformation of CTP to its 3′-deoxy-3′,4′-didehydro analogue. Therefore, promiscuous activity of the fungal enzyme is unique. Our spectroscopic studies using substrate analogues and computational analysis combined with mutagenesis studies revealed new insight into the origin of the substrate promiscuity of TtRSAD2 and the mechanism of dehydration of a nucleotide by the enzyme and its close homologues.

Results and Discussion

Amino acid sequence analysis. We chose to work with TtRSAD2 because of its similarity with the human and mouse antiviral enzyme viperin (RSAD2) (58% identity at the amino acid level). We predicted that TtRSAD2 generates antiviral or antibacterial natural products. Human viperin is shown to be a member of the radical SAM superfamily of enzymes[18–20], which catalyze transformation of a substrate using a common catalytic step (Figure 1a)[21–23]: a highly conserved [4Fe-4S] cluster, which is coordinated to three cysteine residues of a conserved CxxxCxxC motif, cleaves SAM in a one-electron reduction step to generate a 5′-deoxyadenosyl radical (5′-dAdo radical) intermediate[21,24]. The 5′-dAdo radical has recently been trapped

and characterized [25,26] and spectroscopic studies have provided evidence for the formation of an organometallic intermediate with Fe–[5′-C]-deoxyadenosyl bond (Figure 1a)[27,28].

Figure 1

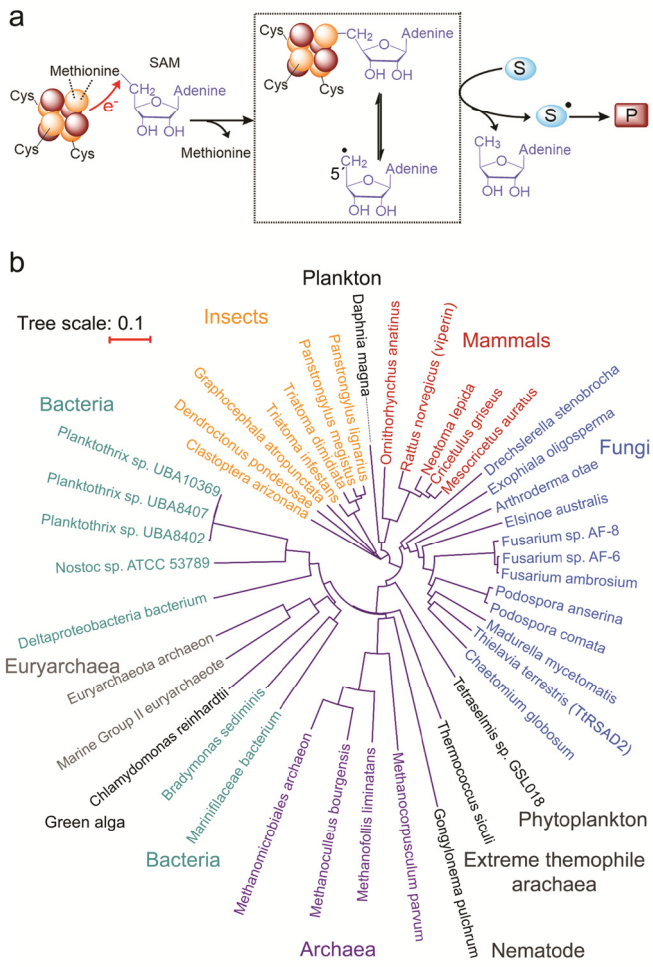

Figure 1. TtRSAD2 is a fungal radical-SAM enzyme with similarity to vertebrate viperin (RSAD2) and has many close relatives in bacteria, archaea, and fungi. (a) The common step in the catalytic transformation of a substrate by most members of the radical-SAM superfamily of enzymes. (b) A rooted phylogenetic tree showing that TtRSAD2 and vertebrate viperin are paralogs. The tree was prepared as explained in the methods.

The organometallic or the 5′-dAdo radical intermediate initiates catalytic transformation by abstracting a hydrogen atom from a substrate, releasing 5′-deoxyadenosine (5′-dA), and generating a substrate-radical intermediate, which undergoes complex rearrangement reactions to form a product[21,24,29,30]. Previously, using EPR spectroscopy and biochemical studies we demonstrated that TtRSAD2 is a radical-SAM enzyme[31,32]. Multiple sequence alignment and phylogenetic analysis revealed that homologues of the enzyme are present in different species of fungi, bacteria, archaea, and green algae (Figure 1b). In all species the CxxxCxxC motif and the GGE motif, which interacts with SAM, are highly conserved (Supplementary Figure 1). The tree shows that vertebrate viperin and TtRSAD2 are paralogs, which have evolved by duplication events. In human viperin, the N-terminus hydrophobic domain consists of approximately 45 amino acid residues, while in TtRSAD2 it is only 22 residues long. The hydrophobic domain presumably anchors the protein into a membrane, like that observed for human viperin[33,34].

Unlike vertebrate viperin, TtRSAD2 has substrate promiscuity. To identify substrates of the enzyme, we first characterized the purified TtRSAD2 using UV-visible and EPR spectroscopies. We confirmed that the enzyme has a [4Fe-4S] cluster (approximately 60-70% of the purified protein as demonstrated in Methods) and can reductively cleave SAM in the absence of a substrate (Supplementary Figure 2). Then, we used HPLC and mass spectrometry to identify different substrates of the enzyme. We measured formation of a product in the presence of a metabolite (Supplementary Figure 3) as compared to four control samples, in each of which a component of the reaction was missing (Methods). We initially screened 19 different metabolites (Supplementary Table 1). We found that CTP, UTP, ATP, and UDP-galactose can all act as substrates for TtRSAD2, as in each case formation of a product was observed (Supplementary Figures 3-4) with concurrent consumption of the substrate and formation of the 5′-dA by-product (Supplementary Figure 4). In the case of CTP and UTP, we used a combination of high-resolution mass spectrometry (Figure 2) and NMR spectroscopy to investigate the molecular structure of the products (Supplementary Figures 5-8). LC-MS confirmed dehydration of CTP and UTP and formation of products (Figure 2). We compared the ^{1}H NMR peaks of the products to those reported for ddhCTP, 3′-deoxy-3′,4′-didehydro-uridine (ddhU), and model compounds (Supplementary Table 2). The data together revealed that in the case of CTP and UTP the enzyme catalyses dehydration of the ribose group, generating nucleotide analogues 3'-deoxy-3′,4'-didehydro-CTP (ddhCTP) (Figure 2a) and 3'-deoxy-3′,4'-didehydro-UTP (ddhUTP) (Figure 2b), respectively. Because the structures of UTP and CTP are very similar, we tested if human viperin, can also catalyse transformation of CTP and UTP. Unlike TtRSAD2, human viperin could only catalyse transformation of CTP to ddhCTP (Supplementary Figure 9). Therefore, we conclude that TtRSAD2 has substrate promiscuity unlike human viperin. Previous isotope labelling experiments using rat viperin led to the conclusion that the 5′-dA radical abstracts H4′ of ribose to catalyze transformation of CTP to ddhCTP[17]. Accordingly, we conclude that in the case of TtRSAD2 the 5′-dA radical intermediate abstracts H4′ of ribose to catalyse transformation of CTP to ddhCTP or UTP to ddhUTP.

Between ATP and UDP-gal, conversion of ATP was significantly higher. High-resolution mass spectrometry (Figure 2c) confirmed that in the case of ATP the product was not formed from the dehydration of ribose. Instead, it was the result of the addition of $(SO_2^{\bullet})^-$ radical ion, present in reactions containing sodium dithionite $(S_2O_4)^{2-}$ as a reducing agent[35], to a radical-intermediate formed from ATP. To determine the position at which the $(SO_2^{\bullet})^-$ radical ion was added, we analysed the fragmentation pattern of the product of catalytic transformation of ATP (Supplementary Figure 10). This approach is an important tool for structural analysis of small molecules[36]. The results narrowed down the position, at which the $(SO_2^{\bullet})^-$ radical ion was added, to the C5′ of the ribose. Addition of $(SO_2^{\bullet})^-$ radical ion to ATP can only occur via a radical-radical cross-coupling mechanism involving a substrate-radical intermediate, as described for other radical-SAM enzymes[37]. Therefore, in the case of ATP, a C5′-centered radical must have been formed by the enzyme. To verify if formation of the radical-intermediate on ATP is catalysed by TtRSAD2, we performed competition studies. In the presence of UTP, CTP, and ATP only UTP was converted to ddhUTP (Supplementary Figure 11). Therefore, UTP is the preferred substrate and binding of ATP to the catalytic pocket in TtRSAD2 is essential for its catalytic transformation. We conclude that in the case of ATP, the 5′-dAdo radical abstracts a hydrogen atom from the C5′ position of ribose generating a C5′-centred radical, which is scavenged by the $(SO_2^{\bullet})^-$ radical ion forming the previously undescribed sulfinic acid derivative (Figure 2c).

Figure 2

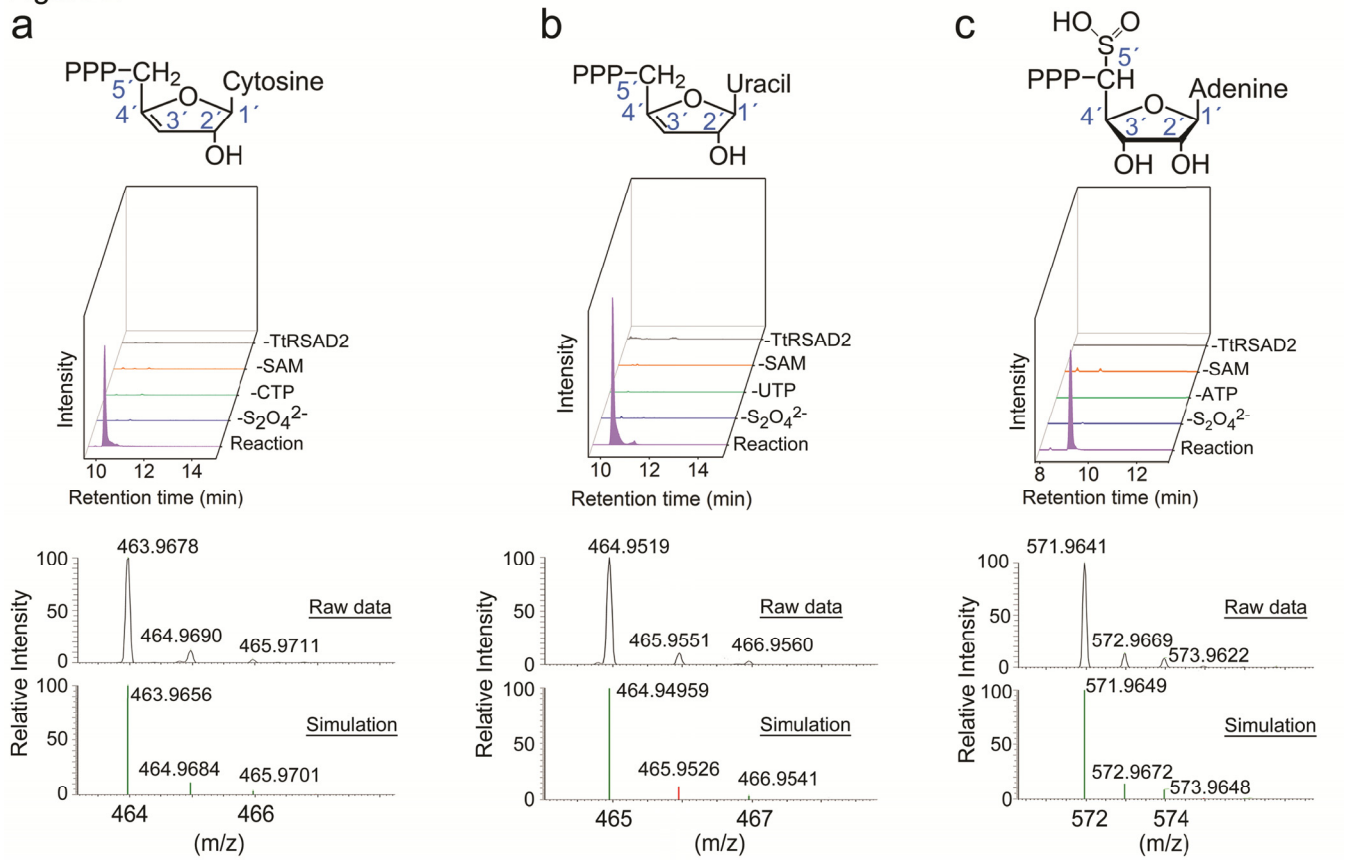

Figure 2. TtRSAD2 has substrate and catalytic promiscuity. (a) High-resolution LC-MS analysis of the formation of ddhCTP $[M-H]^-$, (b) ddhUTP $[M-H]^-$, or (c) sulfinic acid derivative of ATP $[M+H]^+$. On the top are the chromatograms showing formation of (a) ddhCTP, (b) ddhUTP, or (c) sulfinic acid derivative of ATP. Products were only observed when all components of the reaction were present, i.e. the trace marked 'reaction'. Dithionite, $(S_2O_4)^{2-}$, was used as reducing agent to provide the electrons for reductive cleavage of SAM by the [4Fe-4S] cluster. The accurate mass spectrum of the product and a simulation of the spectrum (< 5 ppm error) using the chemical formula of (a) ddhCTP, (b) ddhUTP, or (c) sulfinic acid derivative of ATP are shown under the chromatograms. The structures of ddhCTP and ddhUTP was determined using ^{1}H NMR spectroscopy as explained in the text, and that of the sulfinic acid derivative of ATP was predicted from the fragmentation pattern of the mass spectrum of the product. Measurements were repeated at least two times with different batches of protein.

The difference in the reactivity of ATP compared to CTP or UTP is likely due to the difference between purine and pyrimidine groups. ATP has a bulkier nitrogenous base than UTP or CTP and will consequently have a different orientation in the substrate binding pocket. The difference in the orientation of nucleotides would affect the accessibility of the 5´-dA radical to a specific hydrogen atom resulting in formation of a C5´-centered radical in ATP but C4´-centered radical in UTP and CTP.

Kinetics of ddhUTP and ddhCTP formation. Next, we used HPLC in combination with LC-MS to determine the kinetics of the catalytic transformation of CTP and UTP by TtRSAD2 (Supplementary Figure 12). The specific activity and the apparent K_m value for UTP were (1.5 ± 0.2) x10^{-3} (U/mg, which is µmol of substrate converted per min per mg of enzyme) and 73 ± 4 (µM), respectively, and those for CTP were (0.68 ± 0.04) x10^{-3} (U/mg) and 154 ± 35 (µM), respectively. The kinetic parameters revealed that UTP is the preferred substrate. The finding that the K_m value for UTP is 2-fold less than that for CTP (the binding affinity of UTP is approximately 2-fold higher than that of CTP) and that the specific activity of the enzyme (U/mg) is circa 2.5-fold higher for UTP compared to CTP, is consistent with competition studies (Supplementary Figure 11). Based on competition studies, we found that in the presence of a mixture of UTP, CTP, and ATP, only UTP is efficiently catalysed by the enzyme (Supplementary Figure 11). Nucleoside forms of ddhUTP and ddhCTP, i.e. ddhU and ddhC, have been previously synthesized using chemical methods[38]. Transformation of uridine (U) and cytidine (C) (about 50-90%) to ddhU and ddhC[38], respectively, required multiple protection-deprotection steps. However, using TtRSAD2 the transformation of UTP or CTP (> 95%) to ddhUTP or ddhCTP, respectively, was achieved in a single step.

Hydroxyl groups of ribose induce conformational changes required for catalysis. We sought to test the importance of different functional groups of a nucleotide triphosphate substrate on its binding and reactivity. To this end, we used EPR spectroscopy and probed whether a nucleotide triphosphate can bind to the enzyme and affect the [4Fe-4S] cluster, like the effect observed due to binding of SAM to the enzyme. We tested UTP and ATP as two of the substrates identified by the screening, and four analogues (Figure 3a), namely 5-bromo-UTP, 6-Aza-UTP, ribavirin triphosphate, or zidovudine triphosphate. These analogues were chosen to test the effect of substitution at different positions of UTP on substrate binding. We measured the interaction of a nucleotide in the absence of SAM or its analogue S-adenosylhomocysteine (SAH). This is because binding of SAM or SAH alone would significantly affect the EPR spectrum of the $[4Fe-4S]^{1+}$ cluster (Figure 3), reducing the chance of observing possible changes due to nucleotide binding. Addition of UTP or ATP changed the EPR spectrum of the $[4Fe-4S]^{1+}$ cluster, suggesting structural changes due to their binding (Figure 3b). While addition of 5-bromo-UTP, 6-Aza-UTP, or ribavirin triphosphate in the absence of SAM changed the EPR

spectrum of the [4Fe-4S]$^{1+}$ cluster, addition of zidovudine triphosphate (Figure 3c) did not affect the EPR spectrum of the cluster. Zidovudine triphosphate does not have the hydroxyl groups of ribose and instead has a bulky azido group at the C3´ position. While the presence of a bulky group like azido in zidovudine triphosphate abolished substrate binding and the change on the EPR spectrum of the [4Fe-4S]$^{1+}$ cluster, the presence of a bulky nitrogenous base in ribavirin triphosphate or ATP did not affect binding and the change on the EPR spectrum of the cluster. Therefore, we conclude that the interaction of the hydroxyl groups of ribose with the protein are essential for the conformational changes induced by substrate binding.

Figure 3

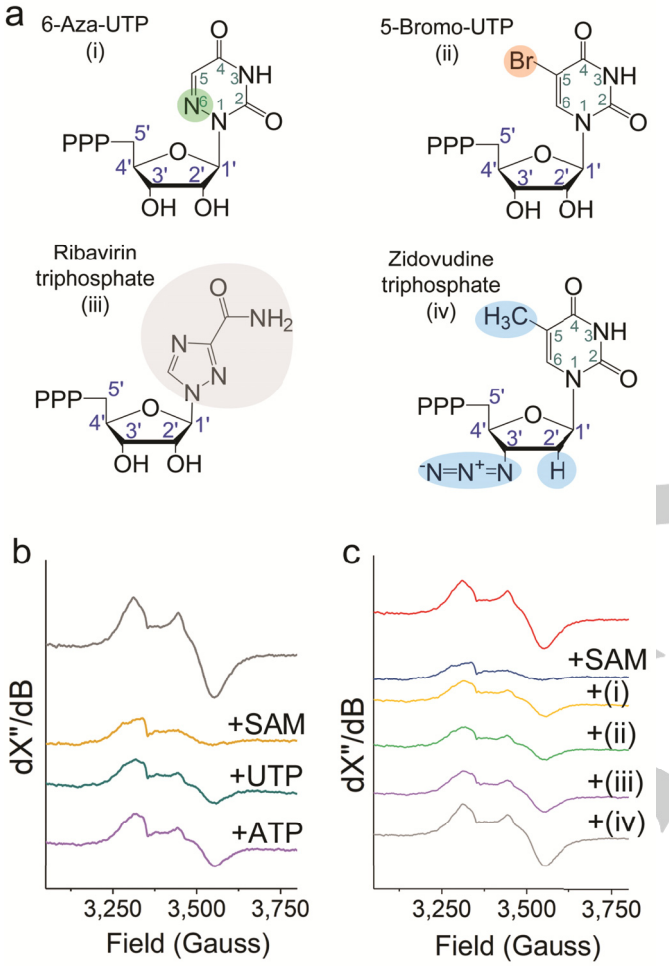

Figure 3. The hydroxyl groups of ribose induce protein conformational changes affecting the EPR spectrum of the [4Fe-4S]$^{1+}$ cluster. (a) Structure of four non-natural nucleotides used to probe substrate binding. The positions that differ from UTP are coloured. (b) Interaction of UTP or ATP in the absence of SAM or (c) non-natural nucleotides (i) 6-Aza-UTP, (ii) 5-boromo-UTP, (iii) ribavirin triphosphate, or (iv) zidovudine triphosphate with TtRSAD2 as measured by EPR spectroscopy. Addition of (iv) zidovudine triphosphate does not alter the EPR spectrum of the [4Fe-4S]$^{1+}$ cluster.

Formation of a tyrosyl radical during reductive dehydration of a nucleotide. In the case of CTP or UTP the C4´-centred radical intermediate must be reduced by an electron to generate the ddhCTP or ddhUTP product (Figure 4a). Transfer of this electron is coupled to the removal of the 3´-hydroxyl group and it most likely originates from a protein amino acid and not the [4Fe-4S] cluster. This is because when H-atom abstraction occurred at the C5´ position of ribose in ATP, the C5´-centered radical could not be reduced by an electron and was scavenged by the $(SO_2^{\bullet})^-$ radical ion generating the sulfinic acid derivative of ATP (Figure 4a). Therefore, we tested if an amino acid-based radical species was formed during the catalytic transformation of UTP. We followed the reaction using EPR spectroscopy after addition of UTP, ATP, 5-bromo-UTP, 6-Aza-UTP, ribavirin triphosphate, or zidovudine triphosphate in the presence of SAM. Addition of UTP but not ATP to the reduced enzyme led to formation of a radical species (Figure 4b).

Figure 4

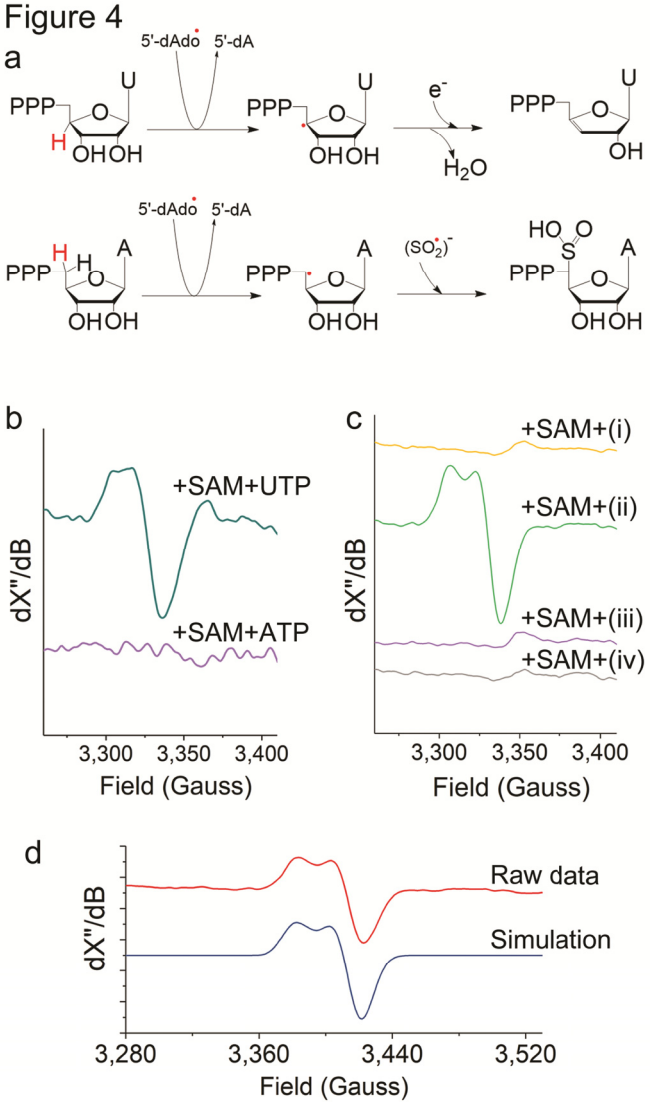

Figure 4. Catalytic dehydration of a nucleotide proceeds via formation of a tyrosyl radical. (a) In the case of UTP an electron is added to the substrate-radical intermediate to form the ddhUTP product, while in the case of ATP an electron cannot be added, and the substrate-radical intermediate is scavenged by a $(SO_2^{\bullet})^-$ radical ion. (b) An amino acid-based radical is formed during the catalytic transformation of UTP but not ATP. (c) The same amino acid-based radical was observed in the presence of 5-bromo-UTP (ii). (b-c) A nucleotide was added in the presence of SAM to the reduced enzyme. EPR spectra were corrected for the background spectrum of the [4Fe-4S]$^{1+}$ cluster in the presence of SAM only. For these experiments the concentration of reducing agent was approximately 5-fold more than the concentration of UTP to provide two electrons required for reductive dehydration and to prevent rapid reduction of radical intermediates. (d) Simulation of the EPR signal observed in the presence of UTP or 5-bromo-UTP. The raw data is that recorded for 5-bromo-UTP. Simulation was performed as explained in the methods and parameters are shown in table 1. EPR conditions are as explained in the methods. Uracil (U) and adenine (A).

Among other nucleotide analogues we tested (Figure 3a), only addition of 5-bromo-UTP led to formation of an EPR species (Figure 4c) like that observed in the presence of UTP. Spin quantification of the EPR signal of the radical (Methods) revealed that the amount of radical species was about 23 μM, which is about 30% of the amount of protein containing one [4Fe-4S] cluster. If the radical we observed by EPR spectroscopy was formed as a result of reductive dehydration of a substrate, TtRSAD2 should have catalysed dehydration of 5-bromo-UTP to the nucleotide analogue 3'-deoxy-3′,4'-didehydro-5-bromo-UTP (5-bromo-ddhUTP). Consistently, HPLC confirmed catalytic conversion of 5-bromo-UTP by the enzyme and NMR spectroscopy (Supplementary Figure 13 and Supplementary Table 2) confirmed the formation of 5-bromo-ddhUTP. It is highly unlikely that we could have trapped the short lived 5´-dAdo radical or a substrate-radical intermediate under steady state conditions. Thus, the most likely origin of the radical is a protein amino acid residue. The EPR signal of the radical is very similar to that of tyrosyl radical in other proteins[39–42]. Additionally, we could simulate (Figure 4d) the spectrum using g-values, line widths, and hyperfine coupling constants similar to those reported for tyrosyl radicals in other proteins (Table 1). It is shown that the environment of tyrosyl radicals affects their EPR parameters[43–45]. Thus, the small variations in the EPR properties of the tyrosyl radical in different enzymes are potentially due to the differences in the environment of the tyrosine radical and hydrogen bonding. Therefore, we conclude that the origin of the radical species we observed is a tyrosine amino acid residue in the catalytic pocket of the enzyme.

Table 1. Comparison of the EPR parameters of the radical in TtRSAD2 with those obtained experimentally or theoretically for tyrosyl radicals in other proteins.

Tyrosyl radical in	g_x, g_y, g_z	W_x, W_y, W_z*	A_x, A_y, A_z **
TtRSAD2 (this work)	2.021, 2.00, 2.00	7.2, 7.7, 7.5	5.5, 7.5, 7.5
Solution[46]	2.01, 2.00, 2.00	----	6.4
***E. coli* RNR**[47]	2.01, 2.00, 2.00	-----	6.6 7.3
Mouse RNR[48]	2.01, 2.00, 2.00	4.5, 3.5, 4.4	9.1, 4.4, 6.6
B. cereus[49]	2.01, 2.00, 2.00	3.4, 3.1, 3.0	9.1, 4.9, 7.9
B. anthracis[50]	2.01, 2.00, 2.00	6.4, 6.3, 4.8	9.1, 4.8, 7.9
S. Typhimurium[51]	2.001, 2.00, 2.00	11.5, 2.5, 7.1	5.8, 5.3, 3.7

*Line widths (gauss); **Hyperfine coupling constants (gauss) of two hydrogen atoms (I=1/2). The hyperfine coupling constants are for H3 and H5. Only for *E. coli* RNR the hyperfine coupling constants are for different H3 and H5. For Tyr• in solution and in *E. coli* RNR the data are for isotropic hyperfine coupling constants. The signs of the hyperfine coupling constants were not determined for TtRSAD2. For other tyrosyl radicals the signs are negative.

Molecular docking and dynamics (MD) simulations. Homology modelling in combination with molecular docking and MD simulations are being exceedingly used to predict and visualize substrate binding to a protein[52,53]. Therefore, we used the X-ray crystal structure of mouse viperin (> 58% identity with TtRSAD2 at the amino acid level) and modelled the structure of TtRSAD2 with more than 95% accuracy[54] (Figure 5a) (Methods). As observed in the X-ray crystal structure of mouse RSAD2, the predicted substrate-binding pocket of TtRSAD2 is connected to the SAM binding site via a channel (Figure 5a). Amino acid residues that form the channel in TtRSAD2 are Asn76, Val108, Asn172, Phe199, Met248, and Tyr252. All these residues are highly conserved (Supplementary Figure 1).

Figure 5

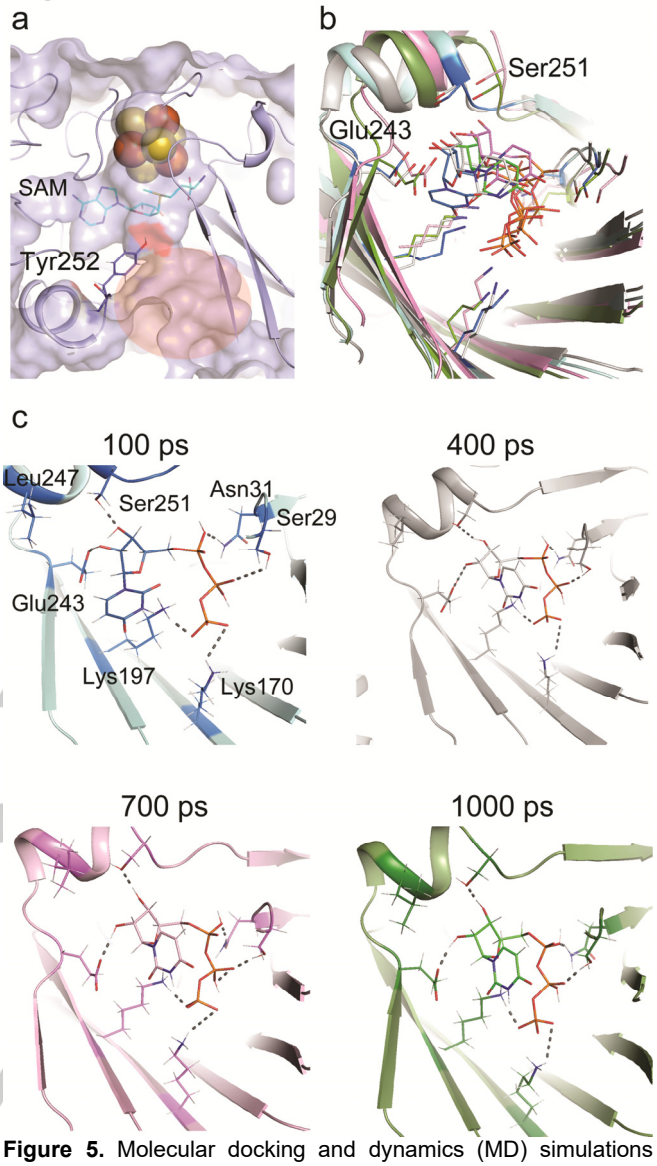

Figure 5. Molecular docking and dynamics (MD) simulations provide insight into substrate promiscuity and binding. (a) The predicted (>95% confidence) structure of TtRSAD2 based on the X-ray crystal structure of mouse RSAD2 (PDB Code: 5VSM). A channel connects the SAM binding pocket to the putative substrate binding pocket (orange oval). A highly conserved tyrosine residue is present in the channel. (b-c) The region of the protein consisting of Glu243 and Ser251, which form hydrogen bonds with the hydroxyl groups of ribose, is very flexible. This region extends to a C-terminal loop. The figure shows the predicted binding pocket of UTP and a series of MD trajectories: blue (100 ps), grey (400 ps), purple (700 ps), and green (1000 ps). The nitrogenous base of UTP is very flexible. The dashed lines show potential hydrogen bonds (distances less than 3 Å).

Tyr252 (Figure 5a) is the only potential amino acid residue in the catalytic pocket that can participate in redox chemistry. It can donate an electron to the substrate-radical intermediate leading to formation of a product and the radical we observed by EPR spectroscopy. Therefore, we sought to estimate the distance of Tyr252 from a substrate. We first used the X-ray crystal structure of mouse viperin and predicted the binding pocket of CTP using molecular docking simulations (Methods). We chose two criteria to identify the best model (Supplementary Figure 14a): (i) the H4´ of ribose in CTP should be pointed toward the SAM allowing its abstraction by 5´-dA radical upon possible conformational

changes as observed by EPR spectroscopy, and (ii) the predicted binding constant should be close to the apparent K_m measured using biochemical studies. We then used molecular docking simulations to predict the binding pocket of UTP in the modelled structure of TtRSAD2 (Supplementary Figure 14b). The results using the X-ray crystal structure of mouse viperin and the modelled structure of TtRSAD2 are the same. The distance of the tyrosine to the ribose group of UTP or CTP is within 5-7 Å and it is within 10 Å from the [4Fe-4S] cluster. Therefore, it is compelling to conclude that Tyr252 donates an electron in a proton-coupled electron transfer step to the C4´-centered radical intermediate to generate a 3'-deoxy-3′,4'-didehydro-nucleotide product, a water molecule, and a tyrosyl radical as observed by EPR spectroscopy. After the $[4Fe\text{-}4S]^{2+}$ cluster is re-reduced, this tyrosyl radical can then be reduced by an electron from the $[4Fe\text{-}4S]^{1+}$ cluster. Consistent with the results of molecular docking simulations, a variant of the enzyme in which Ser251 and Tyr252 were replaced by alanine and phenylalanine, respectively, was fully inactive (Supplementary Figure 15).

To further visualize initial events of substrate binding to TtRSAD2, we performed molecular dynamics simulation using UTP as the substrate (Methods) (Figure 5b-c). The results revealed interesting insight into substrate binding and protein conformational changes: (i) Throughout the course of simulation the 2´-OH and 3´-OH groups of ribose form hydrogen bonds with the highly conserved Glu243 and Ser251, respectively. Additionally, the region of the protein encompassing Glu243 and Ser251 and extending to the C-terminal loop is more flexible as compared to other regions of the protein interacting with the substrate (Figure 5c). During MD simulations, Glu243 and Ser251 moved over a larger distance. This is consistent with our EPR studies using different analogues of UTP showing that the OH groups of ribose induce conformational changes in the protein and thus, affect the EPR spectrum of the [4Fe-4S] cluster. (ii) Ser29, Arn31, Lys170, and Lys197 form hydrogen bonds with the phosphate groups of a nucleotide (Figure 5c). Except, Ser29 all the other residues are highly conserved from TtRSAD2 to the other species (Supplementary Figure 1). (iii) The nitrogenous base of UTP is flexible in its binding pocket (Figure 5b-c). This observation is consistent with our findings based on biochemical studies that the enzyme has substrate promiscuity and is, to some extent, insensitive to the nitrogenous base of a nucleotide. It should be emphasized that our docking and MD simulations are based on structures predicted in the absence of a substrate and thus, the possible conformational changes in the protein after substrate binding are not considered. Therefore, our simulations potentially represent an early stage of substrate binding showing that the interaction of OH groups with the amino acid residues near the C-terminal, i.e. Ser251 and Tyr252 in TtRSAD2, causes the conformational changes required for formation of the final enzyme-substrate complex and catalysis.

Conclusions and mechanistic model

In summary, based on our findings we can draw three main conclusions. (i) The fungal TtRSAD2 has substrate and catalytic promiscuity unlike human viperin. TtRSAD2 catalyses reductive dehydration of UTP, CTP, and 5-bromo-UTP to the nucleotide analogues ddhUTP, ddhCTP, and 5-bromo-ddhUTP via a mechanism requiring a proton-coupled electron transfer step from a tyrosine amino acid residue. The observation that 6-Aza-UTP was not a substrate like UTP or CTP, clearly demonstrates that it is not straightforward to predict a substrate based on similarity of its structure with CTP or UTP. (ii) An amino acid-based radical species is formed only during reductive dehydration of a substrate and this radical most likely originates from the highly conserved Tyr252 in the catalytic pocket. (iii) Substrate binding induces protein conformational changes, which abolish the EPR spectrum of the $[4Fe\text{-}4S]^{1+}$ cluster. The conformational changes are related to the interaction of the OH groups of ribose to a flexible region of the protein consisting of the highly conserved Glu243 and Ser251 and linked to a flexible C-terminal loop. Accordingly, we put forward a working hypothesis for the reductive dehydration of a nucleotide by TtRSAD2. After the initial substrate binding events, which we predicted using molecular docking and MD simulations, conformational changes near the C-terminal induce formation of the final enzyme-substrate complex to initiate catalytic dehydration of substrates (Figure 6). In the proposed mechanism the highly conserved tyrosine provides the electron for the reductive dehydration of a nucleotide in a proton-coupled electron transfer step.

Figure 6

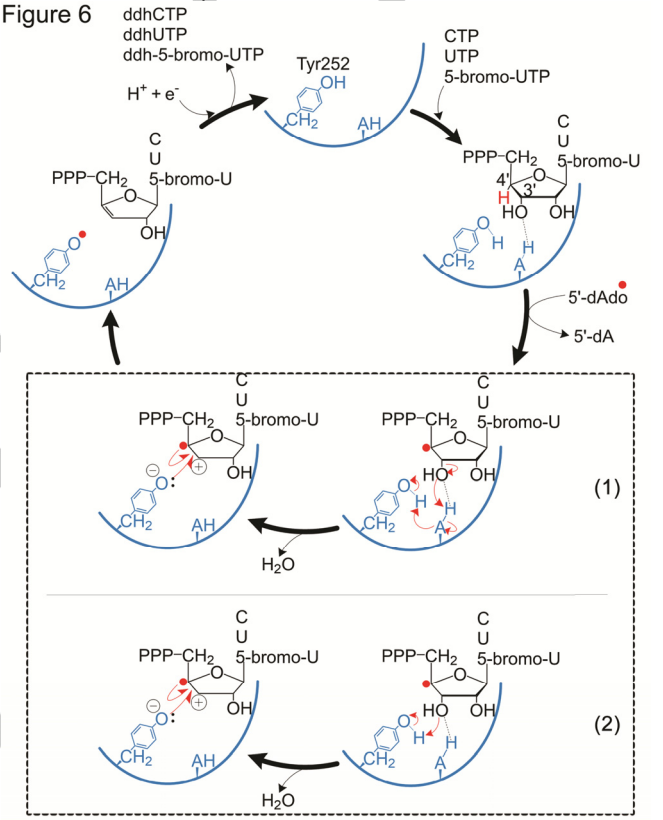

Figure 6. The proposed mechanism of catalysis by TtRSAD2. The 5´-dAdo radical abstracts the H atom (Red) at the C4´ position of ribose to generate a C4´-centered radical intermediate. As a result of hyperconjugation, between a p orbital on C4´ and the σ C3′−O3′ orbital, assisted by a protein amino acid residue (AH), the 3´-OH group of ribose forms a water molecule. The proton to generate the water molecule is provided by tyrosine either indirectly via a proton hopping pathway (1) or directly (2). Spontaneously, an electron from tyrosine reduces the substrate-radical intermediate. As a result, the nucleotide analogue product and a protein tyrosyl radical are formed. The $[4Fe\text{-}4S]^{2+}$ cluster is re-reduced and then, the tyrosyl radical is reduced by an electron from the $[4Fe\text{-}4S]^{1+}$ cluster. Uracil (U), Cytosine (C), and adenine (A). The arrows are based on the conventions used in organic synthesis. The arrow tail is where the electron pair or a single electron starts from. Single barbed arrows show movement of a single electron and double-barbed arrows show movement of electron pairs.

The pathway for transfer of proton from tyrosine remains to be further investigated in detail. Two possibilities can be considered (Figure 6). A proton hopping pathway involving different amino acid residues of the protein. Alternatively, if tyrosine acts as an acid in catalysis, the proton will directly migrate to the OH group

of ribose to form a water molecule (Figure 6). The radical-mediated dehydration of ribose moiety of a nucleotide by TtRSAD2 is not a 1,2-diol dehydration as described for B_{12}-dependent diol dehydratases[55] and the radical-SAM enzyme AprD4[15], which is involved in biosynthesis of amino glycoside antibiotic paramycin. In the case of B_{12}-dependent diol dehydratases a tyrosine amino acid does not participate in catalysis [55]. In the case of AprD4, based on structural and computational studies it is suggested that a tyrosine residue provides an electron for the 1,2-diol dehydration of the sugar moiety in paromamine[15]. We provide direct spectroscopic evidence regarding a proton-coupled electron transfer step in reductive dehydration of ribose by TtRSAD2. Our discovery that TtRSAD2 has substrate promiscuity towards natural and non-natural nucleotides, may suggest a potential role of a similar radical-SAM enzyme in the catalytic transformation and metabolism of antiviral and chemotherapeutic nucleoside analogue cordycepin (3´-deoxyadenosine)[56,57]. Because synthesis of 3´-deoxy nucleotides using enzymatic methods has clear advantages over synthetic methods, our discovery of substrate promiscuity of a thermostable radical-SAM enzyme will unlock the possibility of utilizing the enzyme for synthesis of antiviral, antibacterial, or anticancer nucleotide/nucleoside analogues.

Acknowledgements

KHE is grateful to Prof. Fraser A. Armstrong for his generous support and access to facilities and to Prof. Wilfred R. Hagen (TU Delft, the Netherlands) for providing the financial support to prepare the TtRSAD2 expression construct and conduct experiments with nucleotide analogues, and for discussion of EPR data. We thank Prof. Kylie Vincent (Oxford University) for access to HPLC and for helping with HPLC measurements. We thank Dr Stephen J. Eustace (TU Delft, the Netherlands) for NMR measurements of samples prepared using 5-boromo-UTP. KHE thanks European Molecular Biology Organization (EMBO) (Long-Term Fellowship, ALTF 157-2015), COST (European Cooperation in Science and Technology) Action CA15133 (ECOST-STSM-Request-CA15133-44200), and Edward Penley Abraham Research Fund for financial support. JSR is grateful to Linacre College (Oxford) for an EPA Cephalosporin Junior Research Fellowship.

Conflicts of interest

KHE has applied for a provisional patent application based on the discoveries demonstrated in this manuscript.

Keywords: Radical-SAM• RSAD2 • antiviral • nucleotide analogue • tyrosyl radical

[1] L. P. Jordheim, D. Durantel, F. Zoulim, C. Dumontet, *Nat. Rev. Drug Discov.* **2013**, *12*, 447–464.

[2] E. De Clercq, G. Li, *Clin. Microbiol. Rev.* **2016**, *29*, 695–747.

[3] S. I. Maffioli, Y. Zhang, D. Degen, T. Garzaniga, G. Del Gatto, S. Serina, P. Monciardini, C. Mazzetti, P. Guglierame, G. Candiani, et al., *Cell* **2017**, *169*, 1240–1248.

[4] C. L. Lai, N. Leung, E. K. Teo, M. Tong, F. Wong, H. W. Hann, S. Han, T. Poynard, M. Myers, G. Chao, et al., *Gastroenterology* **2005**, *129*, 528–536.

[5] C. J. Torrance, V. Agrawal, B. Vogelstein, K. W. Kinzler, *Nat. Biotechnol.* **2001**, *19*, 940–945.

[6] A. Fresco-Taboada, I. de la Mata, M. Arroyo, J. Fernandez-Lucas, *Appl. Microbiol. Biotechnol.* **2013**, *97*, 3773–3785.

[7] I. Serra, D. Ubiali, J. Piskur, S. Christoffersen, E. S. Lewkowicz, A. M. Iribarren, A. M. Albertini, M. Terreni, *Chempluschem* **2013**, *78*, 157–165.

[8] J. D. Arco, J. Acosta, H. M. Pereira, A. Perona, N. Lokanath, N. Kunishima, J. Fernandez-Lucas, *ChemCatChem* **2018**, *10*, 439–448.

[9] X. Zhou, K. Szeker, L. Y. Jiao, M. Oestreich, I. A. Mikhailopulo, P. Neubauer, *Adv. Synth. Catal.* **2015**, *357*, 1237–1244.

[10] T. C. Jain, I. D. Jenkins, A. F. Russell, J. P. H. Verheyden, J. G. Moffatt, *J. Org. Chem.* **1974**, *39*, 30–38.

[11] M. J. Robins, R. A. Jones, R. Mengel, *J. Am. Chem. Soc.* **1976**, *98*, 8213–8217.

[12] Y. Ko, M. W. Ruszczycky, S. H. Choi, H. W. Liu, *Angew. Chemie Int. Ed.* **2015**, *54*, 860–863.

[13] X. Ji, Y. Li, W. Ding, Q. Zhang, *Angew. Chemie Int. Ed.* **2015**, *54*, 9021–9024.

[14] M. W. Ruszczycky, Y. Ogasawara, H. W. Liu, *Biochim. Biophys. Acta (BBA)- Proteins Proteomics* **2012**, *1824*, 1231–1244.

[15] W. Q. Liu, P. Amara, J. M. Mouesca, X. Ji, O. Renoux, L. Martin, C. Zhang, Q. Zhang, Y. Nicolet, *J. Am. Chem. Soc.* **2018**, *140*, 1365–1371.

[16] X. Ji, Y. Li, L. Xie, H. Lu, W. Ding, Q. Zhang, *Angew. Chemie* **2016**, *55*, 11845–11848.

[17] A. S. Gizzi, T. L. Grove, J. J. Arnold, J. Jose, R. K. Jangra, S. J. Garforth, Q. Du, S. M. Cahill, N. G. Dulyaninova, J. D. Love, et al., *Nature* **2018**, *558*, 610–614.

[18] K. S. Duschene, J. B. Broderick, *FEBS Lett.* **2010**, *584*, 1263–1267.

[19] B. J. Landgraf, L. McCarthy, Erin, S. J. Booker, *Annu. Rev. Biochem.* **2016**, *85*, 485–514.

[20] N. D. Lanz, S. J. Booker, *Biochim. Biophys. Acta (BBA)-Molecular Cell Res.* **2015**, *1853*, 1316–1334.

[21] J. B. Broderick, B. R. Duffus, K. S. Duschene, E. M. Shepard, *Chem. Rev.* **2014**, *114*, 4229–4317.

[22] M. Fontecave, M. Atta, E. Mulliez, *Trends Biochem. Sci.* **2004**, *29*, 243–249.

[23] J. Wang, R. P. Woldring, G. D. Roman-Melendez, A. M. McClain, B. R. Alzua, E. N. G. Marsh, *ACS Chem. Biol.* **2014**, *9*, 1929–1938.

[24] G. Layer, D. W. Heinz, D. Jahn, W.-D. Schubert, *Curr. Opin. Chem. Biol.* **2004**, *8*, 468–476.

[25] R. I. Sayler, T. A. Stich, S. Joshi, N. Cooper, J. T. Shaw, T. P. Begley, D. J. Tantillo, R. D. Britt, *ACS Cent. Sci.* **2019**, *5*, 1777–1785.

[26] H. Yang, E. C. McDaniel, S. Impano, A. S. Byer, R. J. Jodts, K. Yokoyama, W. E. Broderick, J. B. Broderick, B. M. Hoffman, *J. Am. Chem. Soc.* **2019**, *141*, 12139–12146.

[27] A. S. Byer, H. Yang, E. C. McDaniel, V. Kathiresan, S. Impano, A. Pagnier, H. Watts, C. Denler, A. L. Vagstad, J. Piel, et al., *J. Am. Chem. Soc.* **2018**, *140*, 8634–8638.

[28] M. Horitani, K. Shisler, W. E. Broderick, R. U. Hutcheson, K. S. Duschene, A. R. Marts, B. M. Hoffman, J. B. Broderick, *Science (80-.).* **2016**, *352*, 822–825.

[29] P. A. Frey, A. D. Hegeman, F. J. Ruzicka, *Crit. Rev. Biochem. Mol. Biol.* **2008**, *43*, 63–88.

[30] P. A. Frey, *Annu. Rev. Biochem.* **2001**, *70*, 121–148.

[31] K. Honarmand Ebrahimi, S. B. Carr, J. McCullagh, J. Wickens, N. H.

Rees, J. Cantley, F. Armstrong, *FEBS Lett.* **2017**, *591*, 2394–2405.
[32] K. Honarmand Ebrahimi, C. Silveira, S. Todorovic, *Chem. Commun.* **2018**, 8614–8617.
[33] E. R. Hinson, P. Cresswell, *J. Biol. Chem.* **2009**, *284*, 4705–4712.
[34] E. R. Hinson, P. Cresswell, *Proc. Natl. Acad. Sci.* **2009**, *106*, 20452–20457.
[35] W. G. Hodgson, C. A. Parker, *Nature* **1956**, *178*, 489.
[36] D. P. Demarque, A. E. M. Crotti, R. Vessecchi, J. L. C. Lopes, N. P. Lopes, *Nat. Prod. Rep.* **2016**, *33*, 367–524.
[37] A. Chandor-Proust, O. Berteau, T. Douki, D. Gasparutto, S. Ollagnier-de-Choudens, M. Fontecave, M. Atta, *J. Biol. Chem.* **2008**, *283*, 36361–36368.
[38] M. Petrova, M. Budesinsky, I. Rosenberg, *Tetrahedron Lett.* **2010**, *51*, 6874–6876.
[39] K. Honarmand Ebrahimi, P.-L. Hagedoorn, W. R. Hagen, *ChemBioChem* **2013**, *14*, 1123–1133.
[40] I. Pujols-Ayala, B. A. Barry, *Biochim. Biophys. Acta (BBA)-Bioenergetics* **2004**, *1655*, 205–216.
[41] S. Kim, J. Liang, B. A. Barry, *Proc. Natl. Acad. Sci.* **1997**, *94*, 14406–14411.
[42] B. R. Striet, A. I. Celis, G. C. Moraski, K. A. Shisler, E. M. Shepard, K. R. Rodgers, G. S. Lukat-Rodgers, J. L. DuBois, *J. Biol. Chem.* **2018**, *293*, 3989–3999.
[43] A. Ivancich, T. A. Mattioli, S. Un, *J. Am. Chem. Soc.* **1999**, *121*, 5743–5753.
[44] A. J. Narvaez, L. Kalman, R. LoBrutto, J. P. Allen, J. C. Williams, *Biochemistry* **2002**, *41*, 15252–15258.
[45] M. Lucarini, V. Mugnaini, G. F. Pedulli, M. Guerra, *J. Am. Chem. Soc.* **2003**, *125*, 8318–8329.
[46] R. J. Hulsebosch, J. S. van den Brink, S. A. M. Nieuwenhuis, P. Gast, J. Raap, J. Lugtenburg, A. J. Hoff, *J. Am. Chem. Soc.* **1997**, *119*, 8685–8694.
[47] D. A. Svistunenko, G. A. Jones, *Phys. Chem. Chem. Phys.* **2009**, *11*, 6600–6613.
[48] P. P. Schmidt, K. K. Andersson, A. L. Barra, L. Thelander, A. Graslund, *J. Biol. Chem.* **1996**, *271*, 23615–23618.
[49] A. B. Tomter, G. Zoppellaro, C. B. Bell, A. L. Barra, N. H. Andersen, E. I. Solomon, K. K. Andersson, *PLoS One* **2012**, *7*, e33436.
[50] E. Torrents, M. Sahlin, D. Biglino, A. Graslund, B. M. Sjoberg, *Proc. Natl. Acad. Sci.* **2005**, *102*, 17946–17951.
[51] P. Allard, A. L. Barra, K. K. Andersson, P. P. Schmidt, M. Atta, A. Graslund, *J. Am. Chem. Soc.* **1996**, *118*, 895–896.
[52] J. H. Park, T. Morizumi, Y. Li, J. E. Hong, E. F. Pai, K. P. Hofmann, H. W. Choe, O. P. Ernst, *Angew. Chemie Int. Ed.* **2013**, *52*, 11021–11024.
[53] L. Gelis, S. Wolf, H. Hatt, E. M. Neuhaus, K. Gerwert, *Angew. Chemie Int. Ed.* **2012**, *51*, 1274–1278.
[54] L. A. Kelley, S. Mezulis, C. M. Yates, M. N. Wass, M. J. E. Sternberg, *Nat. Protoc.* **2015**, *10*, 845–858.
[55] D. M. Smith, B. T. Golding, L. Radom, *J. Am. Chem. Soc.* **2001**, *123*, 1664–1675.
[56] K. Nakamura, N. Yoshikawa, Y. Yamaguchi, S. Kagota, K. Shinozuka, M. Kunitomo, *Anticancer Res.* **2006**, *26*, 43–47.
[57] H. S. Tuli, A. K. Sharma, S. S. Sandhu, D. Kashyap, *Life Sci.* **2013**, *93*, 863–869.

Entry for the Table of Contents

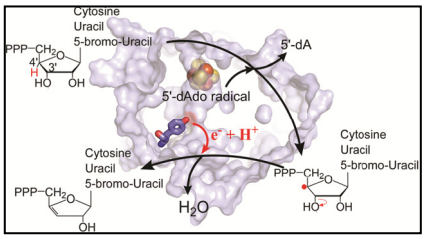

A new fungal radical-SAM enzyme homologue of the human antiviral enzyme can catalyse transformation of a range of natural or non-natural nucleotides to their analogues via a proton-coupled electron transfer mechanism. The enzyme offers new biocatalytic routes for synthesis of 3´-deoxy nucleotides/nucleosides as an important group of antivirals, antibacterial, or anticancer drugs.